Journal of Applied Polymer Science

The Effects on Mechanical Properties and Crystallization of Poly (L-lactic acid) Reinforced by Cellulosic Fibers with Different Scales

Tingju Lu,[1] Man Jiang,[1] Xiaoling Xu,[1] Shengli Zhang,[1] David Hui,[2] Jihua Gou,[3] Zuowan Zhou[1]

[1]Key Laboratory of Advanced Technologies of Materials (Ministry of Education), School of Materials Science and Engineering, Southwest Jiaotong University, Chengdu, People's Republic of China

[2]Department of Mechanical Engineering, University of New Orleans, Louisiana 70148

[3]Department of Mechanical and Aerospace Engineering, University of Central Florida, Florida 32816

Correspondence to: Z. Zhou (E-mail: zwzhou@at-c.net), M. Jiang (E-mail: jiangman1021@163.com) and J. Gou (E-mail: jihua.gou@ucf.edu)

ABSTRACT: Bacterial cellulose (BC), microcrystalline cellulose (MCC), and bamboo cellulosic fibers (BCFs) were used to reinforce poly(L-lactic acid) (PLLA) based bio-composites. The mechanical properties and crystallization of the composites were studied through mechanical testing, differential scanning calorimetry, X-ray diffraction, scanning electron microscopy, and polarizing microscope. The incorporation of all three kinds of cellulose increased the stiffness of the composites compared to pure PLLA. The reinforcing effect of the MCC in the composites is most significant. The Young's modulus and impact toughness of the MCC/PLLA composites were increased by 44.4% and 58.8%, respectively. The tensile strength of the MCC/PLLA composites was increased to 71 MPa from 61 MPa of PLLA. However, the tensile strength of the composites reinforced with BCF or BC was lower than PLLA. The three kinds of cellulosic fibers improved the crystallization of PLLA. The BC with smallest size provided the composites with smallest grain and highest crystallinity. © 2014 Wiley Periodicals, Inc. J. Appl. Polym. Sci. **2014**, *131*, 41077.

KEYWORDS: biomaterials; cellulose and other wood products; composites; crystallization; mechanical properties

Received 8 March 2014; accepted 30 May 2014
DOI: 10.1002/app.41077

INTRODUCTION

The interest to use environmentally friendly materials has increased during the past years because of growing environmental concerns and increasing scarcity of fossil resources.[1,2] Biodegradable polymers like poly(lactic acid) (PLA), polycaprolactone (PCL), and polybutylene succinate (PBS) are promising polymers with high biodegradability and good mechanical properties for industrial applications.[3–5] PLA is made from renewable resources,[6] exhibiting good processability with melting temperatures around 170°C, similar to polypropylene which is one of the most commonly used plastics. On the other hand, the disadvantages of PLA, such as lower impact toughness and low capability of resisting thermal deformation, need to be overcome.[7] The incorporation of reinforcements could improve the impact toughness and thermal stability of PLA.

The biological composite structure of the plant cell wall gives the cells rigidity, strength, and flexibility, which has inspired the exploration of using the main structural component of the cell wall, cellulose, to make bio-based materials that are both useful and renewable.[8] Compared to synthetic counterparts, cellulosic fibers exhibit many advantages such as low density, low cost, high strength-to-weight ratios, easy processing, and especially their renewability and recyclability.[9,10] Significant research has reported the advances in cellulosic fiber reinforced PLA composites, demonstrating better mechanical properties than those of cellulose reinforced PE or PP composites.[11–16]

The varying components and structures of cellulosic fiber may affect the properties of cellulose reinforced PLA composites. Different types of cellulose fillers were reported to make different contributions enhancing the mechanical properties of PLA.[17,18] Bamboo is one of the good resources of cellulose fibers due to its high content of cellulose and relatively small microfibrillar angle.[19] Microcrystalline cellulose (MCC), where the amorphous regions are removed by hydrolysis, can be a promising cellulosic reinforcement of polymers. It is crystalline cellulose derived from high quality wood pulp, and was expected to disintegrated into cellulose whiskers after a completely hydrolysis.[20] MCC has an advantage of high specific surface area over other conventional cellulose fibers.[21] In addition, nanocellulose, which has high mechanical properties, has attracted significant attention in bio-composites.[22,23] The nano-sized cellulose was reported to enhance the properties of the

PLA matrix at a small loading.[8] Bacterial cellulose (BC) is a natural biopolymer and consists of a network of nanofibrils. Compared to other synthetic nanocellulose, BC is a "greener" material because it can be directly produced from bacteria during the culture.[24]

The three kinds of cellulosic fibers with different scales are promising in reinforcing PLA based bio-composites. It is interesting to know which kind of cellulosic fibers has the best performance and how the scale of the cellulosic fibers affects the mechanical and crystalline properties of the composites. However, the discrepancy from the reported results on different cellulosic fibers made it difficult to compare with each other. Lee and Wang reported that the tensile strength increased significantly from 29 MPa to 42 MPa after the filling of bamboo cellulosic fiber (BCF).[25] However, it is reported by Tokoro et al. that BCF slightly decreased the tensile strength of pure PLLA of 86 MPa.[26] For MCC and BC reinforced PLA composites, variations in mechanical properties are found from open literatures.[27–29] Therefore, it is worthy of performing a comparative study in a comprehensive and systematic approach. To our best knowledge, such study has not been conducted yet.

In this study, the BCF, MCC, and BC were used as reinforcement of poly(L-lactic acid) (PLLA) bio-composites. The effects of cellulose loading on the mechanical properties of the PLLA composites were comparatively studied by mechanical testing. Scanning electron microscopy (SEM) and Fourier transform infrared spectroscopy (FTIR) were applied to study the morphologies and structures of the cellulose fibers and composites. The crystallinity and crystalline morphology, which had significant influence on the mechanical and thermal properties of the PLLA composites, were also studied by differential scanning calorimetry (DSC), wide angle X-ray diffraction (WAXD) and polarized optical microscopy (POM).

EXPERIMENTAL

Materials

PLLA (2003D, D-isomer content = 4.3%, $M_w = 2.53 \times 10^5$ g/mol, melt flow rate (MFR) = 4–8 g/10 min (190°C/2.16 kg), and a density of 1.24 g/cm^3) was supplied from Nature Works, USA. The BCF with 95 wt % cellulose content and less than 2 wt % lignin was provided by Sichuan Anxian Paper Co., Ltd. The average values of width and length of the BCF were 8 μm and 500 μm, respectively. The MCC with an average particle diameter of 25 μm was supplied by Aladding Chemistry Co. Ltd. The wet mats of BC were supplied by Membrane Products Technology Co. Ltd. The mat was freeze-dried and smashed with a high-speed universal grinder (FW-400A, 26,000 r/min) for 5 min to be cellulose powder before it was used for the experiments. The diameter of single fiber of BC is about 50 nm. The average values of width and length of the particles of the smashed BC mats are 60 μm.

Preparation of Test Samples of Cellulose/PLA Composites

PLLA composites reinforced by 2 wt % of BCFs, MCCs, and BCs were processed on a mini-extruder (DSM Research, The Netherlands) and a mini-injection molding machine (DSM Research, The Netherlands). The content of the cellulosic fibers in this comparative study was selected to be 2 wt % based on literature study and the results of some exploratory experiments. The BC consisting of a network of nanofibrils was reported to aggregate at a high content. In addition, from the exploratory experiments it was found that the composites filled with 5 wt % cellulosic fibers had similar performance with the composites with 2 wt % fillers. In order to avoid any moisture induced degradation during processing, the cellulose fibers and PLLA were completely dried in the oven. The mini-extruder had three consecutive heating zones and the processing temperatures in these three heating zones (top, center, and bottom) were 180, 175, and 170°C. The screw rotation speed of the micro-extruder was kept at 100 rpm. The PLLA and cellulosic fibers were mechanically mixed and fed into the mini-extruder. After certain processing time in the mini-extruder, the molten mix was transferred to a preheated mini-injection molding machine for the specimen fabrication. The optimized injection pressure to extricate the melt from the cylinder to the mold located in the mini-injection molding machine was 650 kPa at 180°C. Finally, the specimen was removed from the mold for characterization and analysis.

Measurements and Characterizations

Mechanical Tests. The tensile properties were measured on an Instron Universal Tester (Model 3365, AGS-J, Suzhou, China) with a tensile gauge length of 25 mm at the tensile speed of 2 mm/min. The dumbbell-shape samples with the dimensions of 50 mm in length, 3 mm in width, and 3 mm in thickness were analyzed. A pendulum impact tester (XC, Changde, China) was applied to measure the impact strength of the materials. The samples for impact test were 65 mm × 10 mm × 4 mm in three dimensions and a 2 mm deep V-notch was carved on each sample. The values of the mechanical properties of each group were determined by the average value from five tests. The percentage of error as determined by percentage (standard deviation/mean) × 100 was less than 10%.[30]

Scanning Electron Microscopy. Tensile fractural surfaces of the composites were studied by SEM (QUANPA200, The Netherlands) operating in the high vacuum mode at an accelerating voltage of 5 kV. The morphologies of those three kinds of cellulose fibers were characterized by SEM observations. Prior to the examination, the samples were sputtered with gold using JEOL Fine Coater JFC-1200 for 50 s at Argon pressure of 8 Pa and current of 30 mA.

Fourier Transform Infrared Spectroscopy. The chemical structures of BCF, MCC, and BC were analyzed by FTIR. The powders of the three different celluloses were completely dried at 105°C in a drying oven before prepared as KBr pellet and analyzed by FTIR (Nicolet 5700, America) on the sample holder. All spectra were recorded in the wave number range of 400–4000 cm^{-1} with resolution of 4 cm^{-1}.

Wide Angle X-ray Diffraction (WAXD). The crystalline structures of different cellulose fibers and of PLLA in different samples were investigated by using a wide angle X-ray diffraction (WAXD, DX-1000). The continuous scanning angle range used in this study was from 5° to 40° at 35 kV and 25 mA. The powders of different cellulosic fibers were poured onto a glass

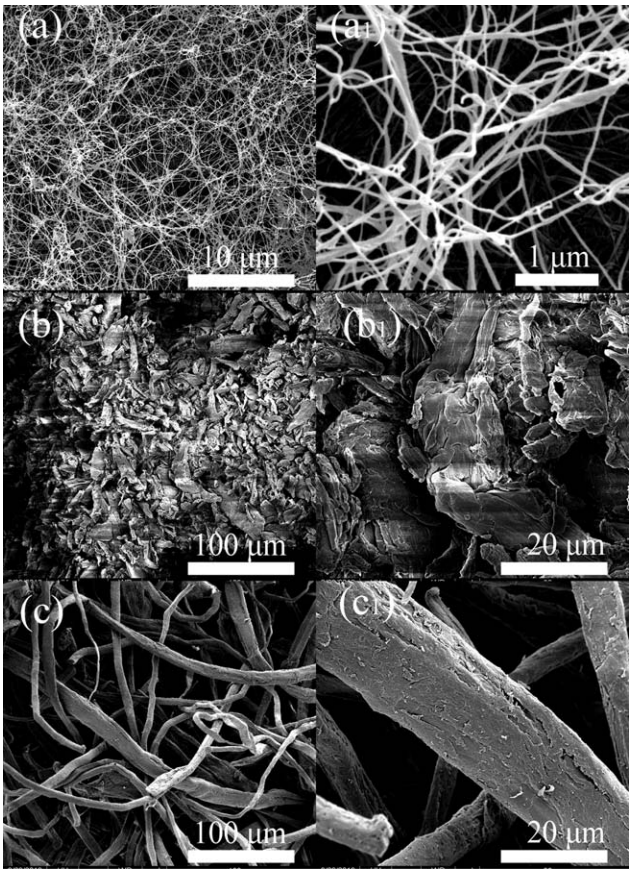

Figure 1. SEM of (a, a_1) BC, (b, b_1) MCC, and (c, c_1) BCF.

holder and pressed to be flat before measurement. For the PLLA composites, the sample was transversely cut and the cross-section was smoothed with sandpaper.

Differential Scanning Calorimetry. The pure PLLA and cellulose/PLLA composites samples were analyzed by DSC using a TA Instruments Q2000 analyzer. Under nitrogen purge, the samples (8 ± 1 mg) contained in aluminum crucibles were heated from 30°C to 200°C, kept at 200°C for 5 min, then cooled down to 30°C, and heated again to 200°C.

Polarized Optical Microscopy. The size and morphology of spherulites of the PLLA composites were observed on a POM (Olympus BX51, Japan) equipped with a charge-coupled device (CCD) camera (HV1301UC, Beijing Daheng, China). A dual-temperature hot stage with a temperature fluctuation of ± 0.1°C was used to control the sample temperature. The film samples of cellulose/PLLA composites with thickness of about 30 μm, sandwiched between two cover glasses, were first melted at 200°C for 5 min to remove the thermal histories. They were quickly transferred to the temperature of 105°C for an isothermal crystallization for 1 h.

RESULTS AND DISCUSSION

Characterizations of Different Celluloses

The microstructure of the reinforcement is important because it ultimately determines the properties of polymer composites. The sizes and surface features of BC, MCC, and BCF were

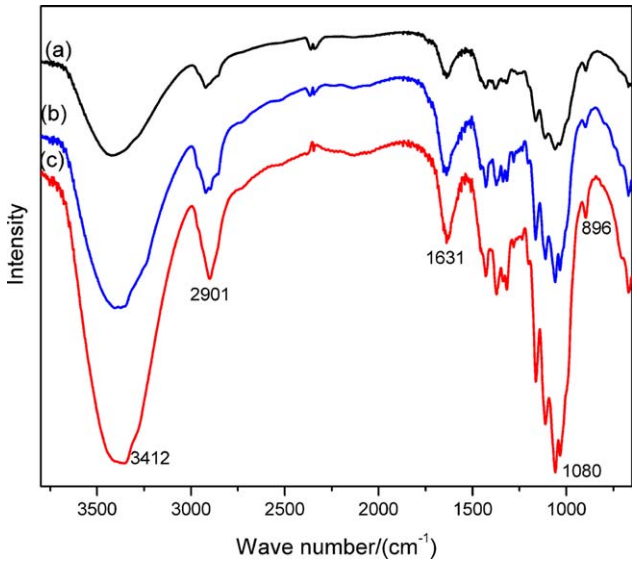

Figure 2. Fourier transform infrared spectroscopy of (a) BC, (b) MCC, and (c) BCF. [Color figure can be viewed in the online issue, which is available at wileyonlinelibrary.com.]

examined by SEM observations, as shown in Figure 1. A well-organized 3D networking structure is shown in Figure 1(a,a_1), which is a typical micrograph of freeze-dried BC. The well-organized fibril network was self-assembled by the bacteria during culture. As shown in Figure 1(a_1), the BC has interconnecting pores and the pore size varies in a certain range. The diameter of a single fiber is about 50 nm. The aspect ratio of the fiber is extremely large, which could provide it with good mechanical properties. It can be seen in Figure 1(b,b_1) that the MCC is in the form of particulate and the particle dimension is in range of 10–25 μm with an aspect ratio of about 1. MCC is the cellulose derived from the high quality wood pulp by an acid hydrolysis to remove the amorphous regions. Therefore, the crystallization and the unity are improved. The shape of MCC is irregular, which could provide it with a large surface area and increase the contact area with the matrix while used in composites. In Figure 1(c,c_1), the BCFs display a fibril form shape with the size around 8 μm in diameter and 400 μm in length. The surface of the BCF is covered with the impurities and/or amorphous cellulose, which could have some negative effects on the properties of the composites.

The FTIR spectra of the three kinds of fibers are shown in Figure 2. Their similar absorption peaks indicated that their ingredient and functional group were almost the same. The peak at 896 cm^{-1} was related to the glycosidic linkages in the cellulose. The band at 3412 cm^{-1} corresponded to the stretching vibration of O—H associated with hydrogen bonds. The absorption at 1080 cm^{-1} was ascribed to aliphatic C—O—C stretching vibration, corresponding to the glucose acetal units in cellulose molecules. The —OH stretching of the bonded water of cellulose and —CH stretching were located at 1631 and 2901 cm^{-1}, respectively.

XRD was used to study the crystalline structures of the samples. The diffraction patterns are shown in Figure 3. The BC

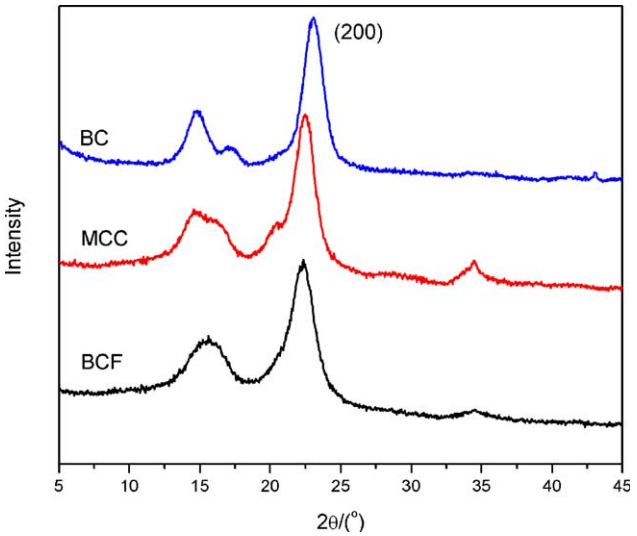

Figure 3. Wide angle X-ray diffraction of (a) BC, (b) MCC, and (c) BCF. [Color figure can be viewed in the online issue, which is available at wileyonlinelibrary.com.]

exhibited three characteristic peaks at 2θ =15.8°, 16.6°, and 24.5°, corresponding to the cellulose I polymorph structure, which was almost identical with the results of Hong and Wang.[31] The BCF and MCC both had diffraction peaks at 2θ =22.5° and 34.5°. For MCC, additional peaks were found at 2θ =15.2° and 16.8°. However, these peaks were not sharp and a shoulder was observed around the region 2θ =14° to 17° for BCF. Based on the diffraction analysis, it was found that the crystalline structure of BCF and MCC were cellulose I structure. The peak at 22.5° of XRD patterns was attributed to the reflections of (200) crystal planes. The crystallinity of cellulose was reflected by crystallinity index (CrI) that could be calculated according to the following relation[31]:

$$\mathrm{CrI}^{\mathrm{XRD}} = \frac{I_{200} - I_{\mathrm{am}}}{I_{200}} \times 100\% \quad (1)$$

where I_{200} is the intensity of peak corresponding to (200), and I_{am} is the intensity of amorphous, usually the lowest peak between 18° and 20°.

The values of CrI were calculated to be 62.8%, 69%, 77.6% for BCF, MCC, and BC, respectively. BC had much higher CrI than the other two. It is believed that the higher the *Cr*I indicates more complete crystalline structure with higher tensile strength.

Mechanical Properties of Cellulose/PLLA Composites

The mechanical properties of the pure PLLA and the composites loaded with different cellulosic fibers are shown in Table I. After being filled with 2 wt % BCF (denoted as PLLA-BCF2), the composites obtained an increase by 22.2% in Young's modulus, which was attributed to the high stiffness of BCF. However, the tensile strength and elongation at break of the PLLA-BCF2 decreased sharply compared to the pure PLLA. Similar results have been reported,[14,16] and the decrease was due to the poor dispersion of cellulose and the poor compatibility between the matrix and the filler. The values of the elongation at break of the virgin PLLA and PLLA composites prepared in this study were much higher than most of ever reported,[21,23] although the incorporation of cellulose fillers decreased it. The impact toughness of the three kinds of composites was significantly improved than those of pure PLLA because of the loose structures of cellulosic fibers which increased the capability of absorbing impact energy.

The BC with 2 wt % loading (denoted as PLLA-BC2) displayed a slight negative effect on the tensile strength and the elongation at break of the composites. This was mainly due to the poor dispersion of the nanosized cellulose fibers in the PLLA matrix, which could be confirmed by SEM micrograph of PLLA-BC2 [Figs. 4(d) and 5 (c_1)]. The BC was fabricated into layered network structures as shown in Figure 1(a), which would be easily aggregated during the mixing procedure. On the other hand, the Young's modulus was improved by adding BC, increased by 28% as compared to the pure PLLA. The impact toughness was increased slightly after the PLLA was filled with BC.

The MCC had commendable impacts on the tensile strength, Young's modulus, and impact toughness, although slightly decreased the elongation at break. The tensile strength was increased from 61 MPa of pure PLLA to 71 MPa of 2 wt % MCC reinforced PLLA (denoted as PLLA-MCC2), with an increase by 16.4%. The Young's modulus and the impact toughness were increased by 44.4% and 58.8%, respectively. Compared to the reported results,[32] the MCC reinforced PLLA composite prepared in this work had better mechanical properties.

The tensile fractures of the cellulose/PLLA composites were observed by SEM to examine the distribution of the cellulose fibers and the interfaces between the fiber and matrix, as shown in Figure 4. From Figure 4(b–d), related to PLLA-BCF2, PLLA-MCC2 and PLLA-BC2, reinforcements could be easily observed. Both small-diameter fibers and lamellar cellulose aggregates could be seen in Figure 4(d), which demonstrated the BC was easily agglomerated and the dispersion of BC in PLLA was poor. Therefore, the BC fabricated by nanocellulose wouldn't enhance the ultimate tensile strength and elongation at break, but slightly decreased them. From Figure 4(b,c), it can be seen that the dispersion of BCF or MCC in PLLA was better than BC. The MCC had smaller size than BCF, indicating the contact area between MCC and PLLA was larger than BCF with the same content. After loading of celluloses, especially for MCC, the tensile fractures of the composites became rougher. The significant deformation of the composite materials indicated that the adding of cellulose fibers increased the capability of energy absorption.

The interfaces between the reinforcements and PLLA are shown in Figure 5. The fractural morphologies of most of the BCFs [Figure 5(a) and (a_1)] were not covered with PLLA, indicating the poor compatibility between the filler and the matrix. Therefore, the BCF could not transfer the loads efficiently, resulting in a decrease in tensile strength. However, some links between the MCC and PLLA were observed in Figure 5(b,b_1). The rough surface of MCC led to increasing the contact area between the filler and the matrix. Therefore, the PLLA resin could tightly bond to the reinforcements. It can be seen in Figure 5(c) that

Table I. Mechanical Properties of PLLA and Its Cellulosic Fibers' Filled Composites

	Young's modulus (GPa)	Tensile strength (MPa)	Elongation at break (%)	Impact toughness (kJ/m^2)
PLLA	1.8 ± 0.1	61 ± 3	16 ± 2	4.25 ± 0.3
PLLA-BCF2	2.2 ± 0.2	53 ± 1	7 ± 1	6.25 ± 0.2
PLLA-BC2	2.3 ± 0.2	57 ± 3	10 ± 2	5.50 ± 0.3
PLLA-MCC2	2.6 ± 0.2	71 ± 2	12 ± 2	6.75 ± 0.4

PLLA: poly(L-lactic acid), PLLA-BCF2: 2 wt % bamboo cellulosic fiber reinforced PLLA, PLLA-BC2: 2 wt % bacterial cellulose reinforced PLLA, PLLA-MCC2: 2 wt % microcrystalline cellulose reinforced PLLA.

some of the BCs with the nanosized fiber were soaked in PLLA. On the other hand, the aggregation of nanocellulose was easily found in Figure 5(c_1).The debonding of two layer of BC could be observed in Figure 5(c_1), which was responsible for poor performance of BC-filled PLLA composites.

Crystallization of Cellulose/PLLA Composites

The crystalline properties of cellulose/PLLA composites were characterized by DSC, WAXD, and POM. The DSC curves of the samples (with a heating rate of 10°C/min) are shown in Figure 6(a), indicating different melting behavior. During the second heating process, the samples exhibited three main transitions: glass transitions at 59°C (T_g), cold crystallization exotherm at 109–120°C (T_{cc}), and melting endotherm at 147–155°C (T_m). Compared to the pure PLLA, the exothermic peak of cellulose reinforced composites shifted to lower temperatures, which was ascribed to the induced crystallization by the fillers. It is interesting to note that the smaller size of the reinforcement is, the lower the temperature for cold crystallization.

Due to the variation in cold crystallization behavior, PLLA exhibited different melting behavior in the samples. The virgin PLLA sample had a main endothermic peak at about 154°C (T_{m2}). For the samples loaded with cellulosic fibers, a shoulder at 148°C (T_{m1}) appeared. It is known that T_{m1} is related to the crystalline structure formed during the cold crystallization process, while T_{m2} is attributed to the melt-recrystallization-melt of PLLA lamellae during the heating process. It can be seen that the T_{m1} shifted to lower temperatures whereas T_{m2} was identical for all the samples. The T_{cc} shifted to lower temperatures with the addition of cellulose. With the decrease of T_{cc}, the chain segments mobility was decreased, which was unfavorable for the growth of lamellae. The smaller the lamellae thickness has, the lower the melt temperature is. Therefore, the T_{m1} decrease with the size of cellulose. However, when the primary lamellae were melted, the chain segments still maintain an ordered structure and then the recrystallization occurred. Since the

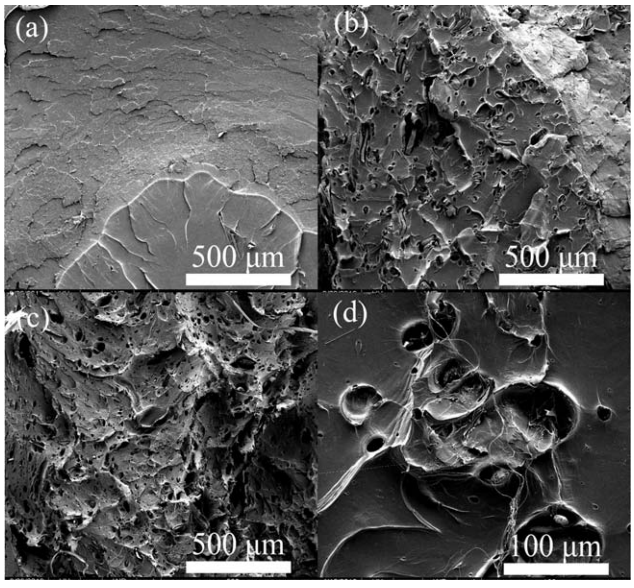

Figure 4. SEM of the tensile fractures of (a) PLLA, (b) 2 wt % BCF reinforced PLLA (PLLA-BCF2), (c) 2 wt % MCC reinforced PLLA (PLLA-MCC2), and (d) 2 wt % BC reinforced PLLA (PLLA-BC2).

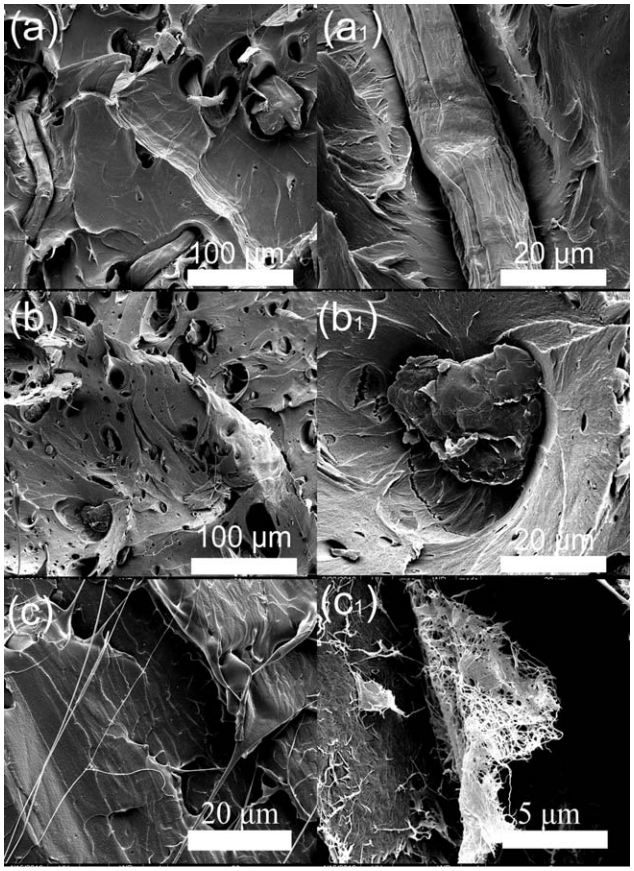

Figure 5. SEM of the tensile fractural morphologies of (a, a_1) PLLA-BCF2, (b, b_1) PLLA-MCC2, and (c, c_1) PLLA-BC2.

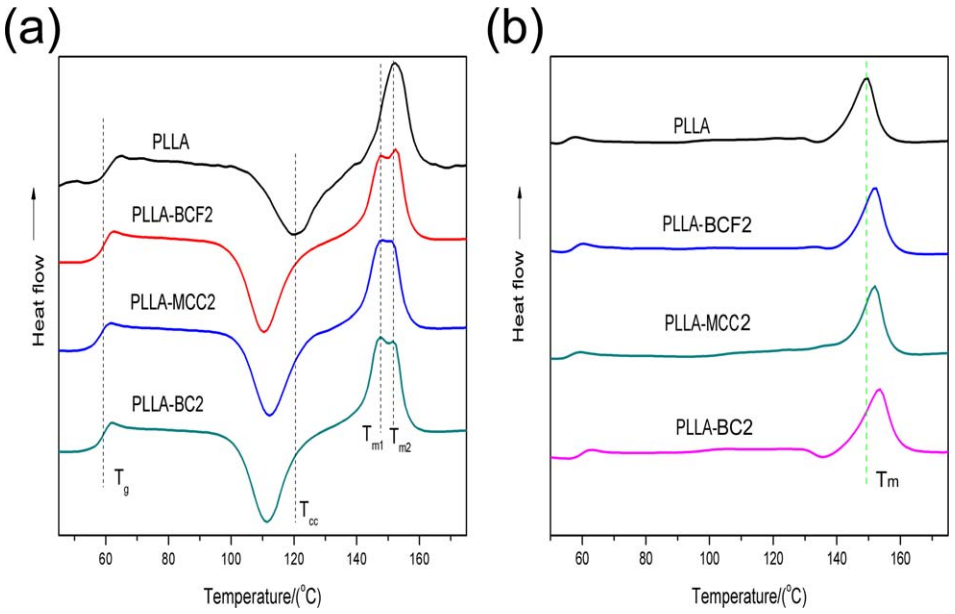

Figure 6. Typical differential scanning calorimeter (DSC) heating curves of the samples (a) after cooled from 200°C to 30°C at 2°C/min, (b) after annealed at 80°C for 12 h. [Color figure can be viewed in the online issue, which is available at wileyonlinelibrary.com.]

recrystallization occurred at almost same temperature, the newly formed lamellae had similar thickness. Therefore, all the samples exhibited the similar T_{m2}.

From the profound cold crystallization exotherm, it is found that the PLLA and cellulose reinforced composites were hardly crystallized due to the rapid de-molding process. To investigate the crystalline structure of PLLA in different composites, the samples were heat-treated to enhance the crystallization. The DSC curves for the samples annealed at 80°C for 12 h [Figure 6(b)] showed no cold crystallization, indicating the high crystallinity of the heat-treated samples. The values of T_g and T_m of cellulose/PLLA composite were slightly higher than those of the pure PLLA. It was ascribed to interactions between the reinforcements and the matrix, which hindered the movements of the segments or molecular chains of PLLA.

The value of X_c of PLLA can be calculated according to the eq. (2) and the results are listed in Table II.

$$X_c = \frac{\Delta H_m - \Delta H_{cc}}{\Delta H_m^0 \times \omega} \times 100\% \quad (2)$$

where ΔH_m (J/g) is the enthalpy of fusion of composites, ΔH_{cc} (J/g) is the enthalpy of cold crystallization of composites, and ω is the weight fraction of PLLA in the composites. ΔH_m^0 is the fusion enthalpy of the completely crystalline PLLA, which is selected as 93 J/g.[33]

Table II. Crystallinity (X_c) of PLLA and Its Composites

Samples	X_c^{XRD} (%)	X_c^{DSC} (%)
PLLA	22.17	17.26
PLLA-BCF2	26.54	19.11
PLLA-MCC2	29.78	17.33
PLLA-BC2	35.86	24.56

The diffraction patterns of PLLA and its composites after annealing at 80°C for 12 h are shown in Figure 7. The sharp and intense diffraction peak at about $2\theta = 16.5°$ was found in all samples, which could be attributed to the reflection of (110)/(200) crystal plane of PLLA. This indicated the presence of crystalline structure in the samples. In other words, cold crystallization occurred during the annealing process, leading to higher crystallinity of PLLA. From the position of (110)/(200) diffraction peak as shown in Figure 7, it can be seen that the annealed PLLA mainly exhibited the α-form crystal. The other diffraction peak, i.e. at $2\theta = 18.8°$, was attributed to the (203) crystal plane of PLLA. The crystallinity of PLLA X_c^{XRD} was calculated according to eq. (3) and summarized in Table II.

$$X_c^{XRD} = \frac{\sum A_{crystalline}}{\sum A_{crystalline} + \sum A_{amorphous}} \times 100\% \quad (3)$$

where $A_{crystalline}$ and $A_{amorphous}$ are the fitted areas from the diffraction peaks of the crystalline and amorphous fractions, respectively.

It can be found that the heat-treated cellulosic fibers-filled samples exhibited higher crystallinity than those of the pure PLLA, which was ascribed to the nucleation of the filled cellulosic fibers during the annealing. From the results of X_c^{XRD}, it can be seen that the smaller size of the filler resulted in higher crystallinity. While the crystallinity of the PLLA-MCC2 characterized by DSC was lower than PLLA-BCF2. The inconsistency in the crystallinity obtained by WAXD and DSC for different composites is possibly due to the high heating rate

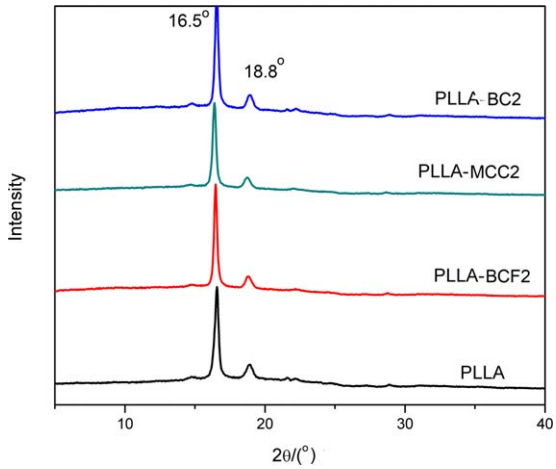

Figure 7. The WXRD of different samples after annealed at 80°C for 12 h. [Color figure can be viewed in the online issue, which is available at wileyonlinelibrary.com.]

to make the crystallinity of PLLA-MCC2 calculated from the DSC test lower than the actual crystallinity. Comparing the isothermal crystallization process of PLLA during heat treatment with the non-isothermal crystallization during DSC test, it can be concluded that cellulose reinforcements could induce the crystallization. However, such effect was sensitive to cooling rate.

In order to inspect the crystalline size and spherulites structures of the PLLA, the samples were examined by POM and the results are shown in Figure 8. The grain of the pure PLLA was nearly 70 μm in diameter. The addition of different cellulosic fibers resulted in disturbing the integrity and lowering the size of the PLLA crystallites. Additionally, the smaller size of the reinforcement is, the smaller the spherulites of PLLA are. The PLLA-BC2 had extremely small grain, about 1/6 as that of the pure PLLA, attributing to the small cellulosic structure of BC which induced crystallization.

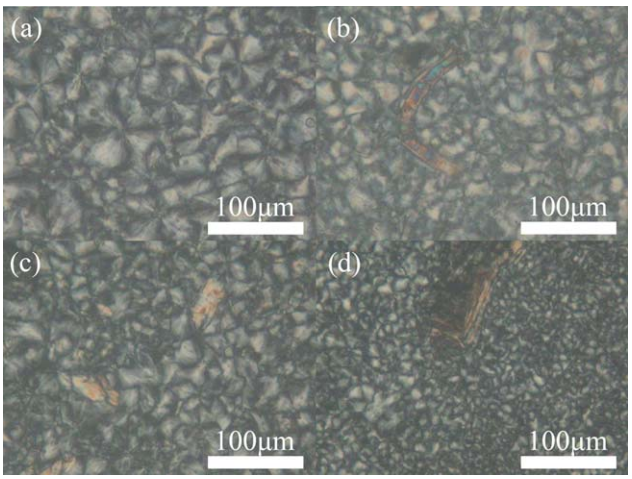

Figure 8. POM graphs of (a) PLLA, (b) PLLA-BCF2, (c) PLLA-MCC2, and (d) PLLA-BC2. [Color figure can be viewed in the online issue, which is available at wileyonlinelibrary.com.]

CONCLUSIONS

The cellulosic fibers reinforced PLLA bio-composites were prepared by filling of BC, MCC, or BCFs. It was found that the incorporation of all the three kinds of cellulosic fibers increased the stiffness of the PLA composites. The MCC with rough surface and large surface area provided the composites with optimal mechanical properties. The decrease in tensile strength of the composites after being filled with bamboo cellulose fiber or BC was mainly due to the poor interfacial adhesion and the poor dispersion of the cellulosic fibers. The three kinds of cellulosic fibers improved the crystallization and refined the grain of PLLA. The smaller the size of the filler resulted in higher crystallinity and smaller spherulites.

ACKNOWLEDGMENTS

This work was financially supported by the National Natural Science Foundation of China (Nos. 51173148, 51303151), National Key Technology R&D Program of the Ministry of Science and Technology of China (No. 2011BAE11B01), Entrepreneurial Talents of Science and Technology Planning Projects of Sichuan Province (No. 2013RZ0036), and the Science and Technology Planning Project of Sichuan Project of Sichuan Province (No. 2011GZX0052).

REFERENCES

1. Zhang, J. F.; Sun, X. Z. *Biomacromolecules* **2004**, *5*, 1446.
2. Seligra, P. G.; Nuevo, F.; Lamanna, M.; Fama, L. *Compos. Part B* **2013**, *46*, 61.
3. Koo, G. H.; Jang, J. *J. Appl. Polym. Sci.* **2013**, *127*, 4515.
4. Liang, J. Z.; Zhou, L.; Tang, C. Y.; Tsui, C. P. *J. Appl. Polym. Sci.* **2013**, *128*, 2940.
5. Garlotta, D. *J. Polym. Environ.* **2001**, *9*, 63.
6. Detyothin, S.; Selke, S. E.; Narayan, R.; Rubino, M.; Auras, R. *Polym. Degrad. Stab.* **2013**, *98*, 2697.
7. Yussuf, A. A.; Massoumi, I.; Hassan, A. *J. Polym. Environ.* **2010**, *18*, 422.
8. Wang, T.; Drzal, L. T. *ACS Appl. Mater. Interfaces* **2012**, *4*, 5079.
9. Odonnell, A.; Dweib, M. A.; Wool, R. P. *Compos. Sci. Technol.* **2004**, *64*, 1135.
10. Ku, H.; Wang, H.; Pattarachaiyakoop, N.; Trada, M. *Compos. Part B* **2011**, *42*, 856.
11. Sharma, M. C.; Hamad, W. Y. *Cellulose* **2013**, *20*, 2221.
12. Alam, A. K. M.; Beg, M. D. H.; Reddy Prasad, D. M.; Khan, M. R.; Mina, M. F. *Compos. Part A* **2012**, *43*, 1921.
13. Oksman, K.; Skrifvars, M.; Selin, J. F. *Compos. Sci. Technol.* **2003**, *63*, 1317.
14. Suryanegara, L.; Nakagaito, A. N.; Yano, H. *Cellulose* **2010**, *17*, 771.
15. Vozzi, G.; Corallo, C.; Daraio, C. *J. Appl. Polym. Sci.* **2013**, *129*, 528.
16. Jiang, A. J.; Xi, J. L.; Wu, H. W. *J. Reinf. Plast. Compos.* **2012**, *31*, 621.

17. Mathew, A. P.; Oksman, K.; Sain, M. *J. Appl. Polym. Sci.* **2005**, *97*, 2014.
18. Bajpai, P. K.; Singh, I.; Madaan, J. *J. Reinf. Plast. Compos.* **2012**, *31*, 1712.
19. Okubo, K.; Fujii, T.; Thostenson, E. T. *Compos. Part A* **2009**, *40*, 469.
20. Haafiz, M.; Hassan, A. *Carbohydr. Polym.* **2013**, *98*, 139.
21. Pei, A.; Zhou, Q.; Berglund, L. A. *Compos. Sci. Technol.* **2010**, *70*, 815.
22. Jonoobi, M.; Harun, J.; Mathew, A. P.; Oksman, K. *Compos. Sci. Technol.* **2010**, *70*, 1742.
23. Lee, K. Y.; Tang, M.; Williams, C. K.; Bismarck, A. *Compos. Sci. Technol.* **2012**, *72*, 1646.
24. Feldmann, E. M.; Sundberg, J. F.; Bobbili, B.; Schwarz, S.; Gatenholm, P.; Rotter, N. *J. Biomater. Appl.* **2013**, *28*, 626.
25. Lee, S. H.; Wang, S. Q. *Compos. Part A* **2006**, *37*, 80.
26. Tokoro, R.; Vu, D. M.; Okubo, K.; Tanaka, T.; Fujii, T.; Fujiura, T. *J. Mater. Sci.* **2008**, *43*, 775.
27. Serizawa, S.; Inoue, K.; Iji, M. *J. Appl. Polym. Sci.* **2006**, *100*, 618.
28. Sabo, R.; Jin, L.; Stark, N.; Ibach, R. E. *BioResources* **2013**, *8*, 3322.
29. Lee, K.-Y.; Blaker, J. J.; Bismarck, A. *Compos. Sci. Technol.* **2009**, *69*, 2724.
30. Lu, T. J.; Liu, S. M.; Jiang, M.; Zhou Z. W. *Compos. Part B* **2014**, *62*, 191.
31. Hong, L.; Wang, Y. L. *Mater. Lett.* **2006**, *60*, 1710.
32. Aji, P.; Mathew, K. O.; Sain, M. *J. Appl. Polym. Sci.* **2005**, *97*, 2014.
33. Watanabe, K.; Tabuchi, M.; Morinaga, Y.; Yoshinaga, F. *Cellulose* **1998**, *5*, 187.